

# Fluorescence and phosphorescence from individual $C_{60}$ molecules excited by local electron tunneling

Elizabeta Cavar,<sup>1</sup> Marie-Christine Blum,<sup>1</sup> Marina Pivetta,<sup>1</sup>  
Francois Patthey,<sup>1</sup> Majed Chergui,<sup>2</sup> and Wolfdieter Schneider<sup>1</sup>

<sup>1</sup>Ecole Polytechnique Fédérale de Lausanne (EPFL),  
Institut de Physique des Nanostructures, CH-1015 Lausanne, Switzerland

<sup>2</sup>Ecole Polytechnique Fédérale de Lausanne (EPFL),  
Laboratoire de Spectroscopie Ultrarapide, ISIC, CH-1015 Lausanne, Switzerland  
(Dated: March 23, 2024)

Using the highly localized current of electrons tunneling through a double barrier Scanning Tunneling Microscope (STM) junction, we excite luminescence from a selected  $C_{60}$  molecule in the surface layer of fullerene nanocrystals grown on an ultrathin NaCl film on Au(111). In the observed luminescence, fluorescence and phosphorescence spectra, pure electronic as well as vibronically induced transitions of an individual  $C_{60}$  molecule are identified, leading to unambiguous chemical recognition on the single-molecular scale.

PACS numbers: 68.37.Ef, 73.20.Mf, 73.22.-f

Light emission induced by electrons tunneling through the junction formed by the sample and the tip of a Scanning Tunneling Microscope (STM) has been proposed to characterize the optical properties of nanoscale objects at surfaces [1]. Contrary to conventional non-local techniques, the local character of this method offers the unique possibility to select and probe individual atoms, molecules or clusters on surfaces.

Photon emission due to the decay of localized surface plasmons, excited by inelastic electron tunneling (IET) has been observed on metal surfaces [2, 3], as well as on supported metallic nanoparticles [4]. Luminescence spectra have been acquired from semiconductor heterostructures [5], quantum well states of metallic films [6]. Recently, luminescence from supported molecules has been obtained [7, 8] by successfully decoupling them from the metallic substrate in order to avoid quenching of the radiative transitions [9, 10], using either a thin oxide film [7] or several molecular layers [8].

However, unambiguous chemical identification of single complex molecules requires the observation and identification of several vibrational and/or electronic-vibrational transitions, which are the spectroscopic fingerprint of the species. Here we present the first observation of energy resolved luminescence from an individually selected  $C_{60}$  molecule excited by electrons tunneling through a double barrier STM junction. A comparison with the luminescence spectra obtained by non-local laser spectroscopy from dispersed  $C_{60}$  molecules in rare gas and glass matrices [11, 12, 13, 14, 15, 16], and from solid  $C_{60}$  [17, 18, 19] enables us to demonstrate the molecular origin of the detected light and to identify the observed spectral features with pure electronic transitions and with vibronic transitions induced via Jahn-Teller (JT) and Herzberg-Teller (HT) coupling [20, 21]. The present novel observation of both, fluorescence (singlet-to-singlet transitions) and phosphorescence (triplet-to-

singlet transitions) constitutes a solid basis for the chemical identification of an individual  $C_{60}$  molecule.

$C_{60}$  nanocrystals were grown on NaCl layers deposited onto a Au(111) substrate. NaCl was evaporated from a Knudsen cell on a clean Au(111) surface at room temperature. Subsequently, the  $C_{60}$  molecules were sublimated on the NaCl covered substrate. The experiments were performed with a homebuilt ultrahigh vacuum (UHV) STM operating at a temperature of 50 K, using cut PtIr tips. The photons emitted from the tunnel junction were collected by a lens placed inside the cryostat, guided through an optical system outside the UHV chamber to the spectrograph, and detected by a CCD camera. The wavelength resolution of the experiment was 8 nm, corresponding to 20 meV in the energy range of interest. The spectra were acquired with closed feedback loop while tunneling over a defined position on the sample, e.g. over a single molecule, with a typical acquisition time of 300 s. Bias voltages  $V$  refer to the sample voltage with respect to the tip.

NaCl forms (100)-terminated islands on Au(111) of thickness between 1 and 3 monolayers and width up to 1  $\mu\text{m}$ . Contrary to the layer-by-layer growth of  $C_{60}$  on Au(111) leading to extended islands found by STM [22], on NaCl electron microscopy studies [23] revealed that the  $C_{60}$  molecules aggregate into hexagonal or truncated triangular nanocrystals with a height of several molecular layers. This situation is well illustrated in Fig. 1, where  $C_{60}$  islands grown on both, the bare Au(111) (A) and the NaCl covered surface (B-D) are visible. The nanocrystals present a minimum height of two layers of  $C_{60}$  molecules (island B). The nucleation of the  $C_{60}$  nanocrystals starts at defects of the NaCl layer (protrusions or vacancies), monatomic steps of Au(111) (covered with NaCl), or edges of the second layer of NaCl. As shown in Fig. 1(b), the  $C_{60}$  molecules form hexagonally arranged layers with an intermolecular distance of 1 nm.

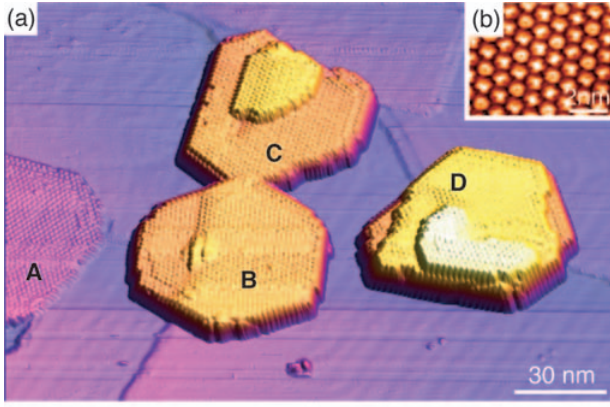


FIG. 1: (color online). (a) STM image of  $C_{60}$  nanocrystals formed on a NaCl ultrathin film grown on Au(111) ( $V = -3V$ ,  $I = 0.02 \text{ nA}$ ). Island A is a  $C_{60}$  monolayer on Au(111), the small blue triangle below A is part of the bare Au surface. Hexagonal island B, and truncated triangular islands C and D consist of up to two, three, and four  $C_{60}$  molecular layers, respectively, on NaCl. (b) Sub-molecular resolution on island B ( $V = -3V$ ,  $I = 0.1 \text{ nA}$ ).

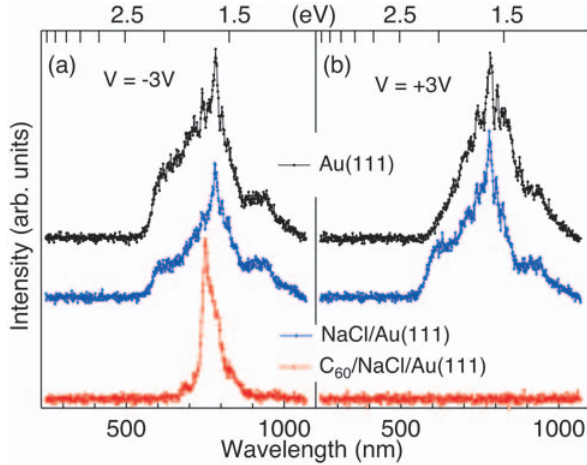


FIG. 2: (color online). STM-induced photon emission spectra acquired with (a) negative ( $V = -3V$ ,  $I = 1 \text{ nA}$ ) and (b) positive ( $V = +3V$ ,  $I = 1 \text{ nA}$ ) bias polarity. Spectra acquired on bare Au(111) and on NaCl thin film reveal characteristic emission from a localized surface plasmon. Emission from  $C_{60}$  can only be excited at negative voltages. Spectra are vertically shifted for clarity.

Figure 2 shows STM-induced optical spectra from the bare Au(111) surface, the NaCl covered Au(111) surface and from a  $C_{60}$  nanocrystal. Photons emitted from Au(111) originate from an IET process, involving excitation and decay of a surface plasmon localized between the tip and the surface [2, 3, 24]. A similar spectral shape is observed over the NaCl layer, however with reduced intensity due to the dielectric NaCl spacer layer. Char-

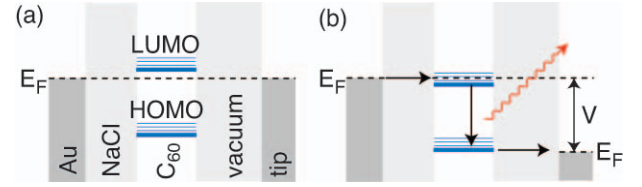


FIG. 3: (color online). Energy diagram of the double barrier tunneling junction at (a) at zero-bias voltage, (b) applied negative voltage, corresponding to the conditions for luminescence.

acteristic for this process is the energy-dependent quantum cut-off [2] (not shown) and the possibility to excite the emission with both bias polarities [3], as shown in Fig. 2. The third spectrum in Fig. 2(a) was acquired over a single  $C_{60}$  molecule in the surface of a nanocrystal ( $V = -3V$ ,  $I = 1 \text{ nA}$ ). Light emission from  $C_{60}$  is observed only for bias higher than the threshold voltage of  $V = 2.3V$ . The emission onset is located at 680 nm and its position is independent of the voltage. For positive voltages up to +4.5 V no photon emission is detected. These observations clearly distinguish the light emission spectrum of  $C_{60}$  from those acquired over the substrate (Au and NaCl).

The occurrence of luminescence from the  $C_{60}$  molecule is related to the characteristics of the tunneling junction, as shown in Fig. 3. At negative bias voltage larger than 2.3 V, the highest-occupied molecular orbital (HOMO), which is completely filled for  $C_{60}$  in the ground state, is higher than the Fermi level ( $E_F$ ) of the tip. The electrons are extracted from the HOMO and tunnel to the tip, while the lowest-unoccupied molecular orbital (LUMO), now lower than the Fermi level of the sample, is populated by the electrons tunneling from the substrate, electrons that can radiatively decay into the partially empty HOMO (hot electron/hole injection). The fact that luminescence is not observed for tunneling from the tip to the sample for voltages up to +4.5 V may be due to the asymmetry of the HOMO-LUMO gap with respect to  $E_F$  [25] and to the different properties of the two tunneling barriers (vacuum and NaCl) [26].

Figure 4(a) shows the same luminescence spectrum obtained from an individual  $C_{60}$  molecule as in Fig. 2(a), but corrected for the quantum efficiency of the detection system. In order to identify the electronic and vibronic transitions giving rise to the observed emission, we compare our results with laser-induced high-resolution photoluminescence data [13, 14] and with quantum chemical calculations [14, 21]. It is now established that the lowest excited singlet state  $S_1$  has mixed  $T_{1g}$ ,  $T_{2g}$  and  $G_g$  character [14]. The electric dipole transitions from this state to the ground state  $S_0$  ( $A_g$ ) are symmetry forbidden, but they occur through HT and JT electron-vibration coupling mechanisms of intensity borrowing [20, 21]. The relaxation of the selection rules due to symmetry lower-

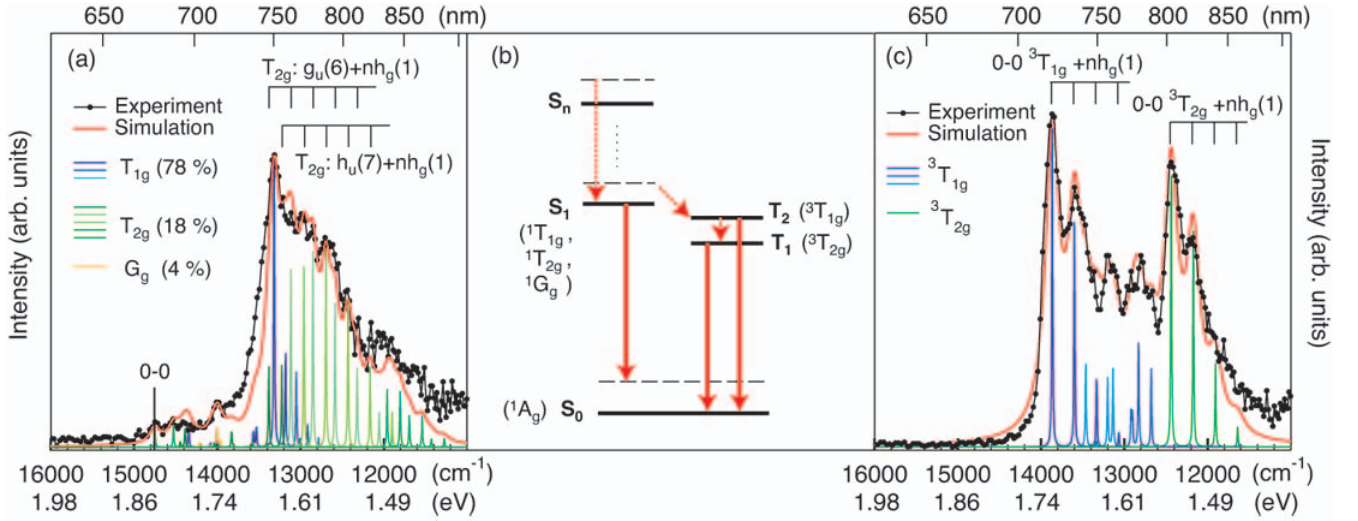


FIG. 4: (color online) (a) STM-induced light emission spectrum assigned to C<sub>60</sub> uorescence ( $V = 3\text{V}$ ,  $I = 1\text{nA}$ ) and calculated spectrum. (b) Schematic diagram of the lowest singlet ( $S_1$ ) and triplet ( $T_1$ ) states. Horizontal solid lines: pure electronic levels; horizontal dashed lines: vibrational levels. Solid arrows represent electronic transitions; dashed arrows represent radiationless mechanisms of relaxation (internal conversion, intersystem crossing, vibrational relaxation). (c) STM-induced light emission spectrum assigned to C<sub>60</sub> phosphorescence ( $V = 3\text{V}$ ,  $I = 1\text{nA}$ ) and calculated spectrum. For both simulations, experimentally determined frequencies for the vibronically induced  $S_0 \rightarrow S_1$  ( $T_{1g}$ ,  $T_{2g}$ ,  $G_g$ ) and  $S_0 \rightarrow T_1$  ( ${}^3T_{2g}$ ,  $T_2$  ( ${}^3T_{1g}$ )) transitions are used, see Tab. I [14, 27]. Each component has a Lorentzian lineshape, broadened by  $150\text{ cm}^{-1}$  (a) and  $200\text{ cm}^{-1}$  (c) to obtain the calculated spectra (red).

TABLE I: HT and JT active modes used in the simulation of the STM-induced light emission spectra shown in Fig. 4 (a,c). For the most intense modes contributing to the spectra, the experimental frequencies [14, 27] are indicated in brackets.

Fluorescence: $S_0 \rightarrow S_1$		Phosphorescence: $S_0 \rightarrow T_1, T_2$
$S_1$ ( $T_{1g}$ )	HT: $t_{1u}$ (4) ( $1430\text{ cm}^{-1}$ ), $h_u$ (7) ( $1566\text{ cm}^{-1}$ ), $h_u$ (1), $h_u$ (3), $h_u$ (4), $t_{1u}$ (3), $h_u$ (5). JT: $h_g$ (7), $a_g$ (2), $h_g$ (1).	$T_1$ ( ${}^3T_{2g}$ ) JT: $h_g$ (1) ( $266\text{ cm}^{-1}$ ).
$S_1$ ( $T_{2g}$ )	HT: $g_u$ (6) ( $1410\text{ cm}^{-1}$ ), $h_u$ (7) ( $1566\text{ cm}^{-1}$ ), $g_u$ (1), $h_u$ (1), $g_u$ (4), $h_u$ (5). JT: $h_g$ (1) ( $266\text{ cm}^{-1}$ ), $h_g$ (7), $a_g$ (2).	$T_2$ ( ${}^3T_{1g}$ ) HT: $t_{2u}$ (3) ( $1037\text{ cm}^{-1}$ ), $h_u$ (1), $h_u$ (2), $h_u$ (4), $a_u$ (1), $g_u$ (4), $t_{1u}$ (3). JT: $h_g$ (1) ( $266\text{ cm}^{-1}$ ).
$S_1$ ( $G_g$ )	HT: $h_u$ (4) ( $738\text{ cm}^{-1}$ ), $h_u$ (2), $h_u$ (3), $g_u$ (3), $g_u$ (5), $t_{2u}$ (2).	

ing in the C<sub>60</sub> lattice gives rise to a very weak luminescence signal corresponding to the pure electronic ( $0-0$ )  $S_0 \rightarrow S_1$  transition, found at  $678\text{ nm}$ , as indicated in Fig. 4 (a). The red shift of about  $40\text{ nm}$  with respect to C<sub>60</sub> in the gas phase is attributed to environmental effects [13, 14, 16]. The observation of the pure electronic origin helps to determine the vibronically induced false origins as in the high-resolution photoluminescence measurements [11, 14]. The uorescence spectra are simulated using calculated oscillator strengths and experimentally determined frequencies for the HT vibronically induced  $S_0 \rightarrow S_1$  ( $T_{1g}$ ,  $T_{2g}$ ,  $G_g$ ) transitions, and the experimental frequencies for the JT active modes, as presented in Fig. 4 (a) and in Tab. I [14, 27]. The contribution of each symmetry character of  $S_1$  varies slightly from one probed molecule to another, reflecting the known

sensitivity of C<sub>60</sub> to the local environment [14, 18, 28]. The agreement between measured and calculated spectra in Fig. 4 (a) demonstrates the local character of the measurement and provides evidence for the preservation of the C<sub>60</sub> molecular properties in the van de Waals crystal, characterized by weak interactions between the molecules.

Interestingly, we also observe another type of electronic transitions, shown in Fig. 4 (c). Similar spectra have been reported for laser-induced luminescence from solid C<sub>60</sub> [17, 18, 19], and have recently been identified as phosphorescence originating from triplet to singlet ground state transitions [28]. Although symmetry and spin-forbidden, intense pure electronic ( $0-0$ ) triplet to singlet transitions have been observed in C<sub>60</sub> phosphorescence spectra [12, 15]. The low-energy part of the spectrum

in Fig. 4(c) arises from the  $S_0 \rightarrow T_1$  ( $^3T_{2g}$ ) transition, characterized by the intense 0-0 origin at 803 nm and by the progression of a JT active mode, see Tab. I, in agreement with phosphorescence spectra obtained from dispersed  $C_{60}$  molecules [11, 12, 15]. The electronic origin is shifted by 27 nm to the red with respect to the estimated gasphase energy [12, 28]. The high-energy region of the spectrum presents a similar shape, i.e. an intense transition, located at 720 nm, and a progression of vibronic bands. The observed energy difference of

0.18 eV between the two most intense features in the spectrum shown in Fig. 4(c) is in agreement with electron energy loss spectroscopy results [28, 29] and with calculations [30] for the splitting of the lowest  $C_{60}$  triplet states. Therefore, the high-energy part of the spectrum in Fig. 4(c) is assigned to transitions from the next higher triplet state  $S_0 \rightarrow T_2$  ( $^3T_{1g}$ ) [28]. The good agreement between the calculated and the measured spectra allows us to assign the STM-induced phosphorescence spectrum to light emission from an individual  $C_{60}$  molecule, as in the case of fluorescence. This finding contradicts previous interpretations of similar spectra obtained by laser induced luminescence from solid  $C_{60}$  in terms of excitonic emission [17] or emission delocalized over more than one  $C_{60}$  molecule [18, 19].

The observation of both radiative relaxation processes, fluorescence and phosphorescence, in the STM-induced light emission may be related to (i) the sensitivity of the probed  $C_{60}$  molecule to the local environment in the nanocrystal and/or to (ii) the actual tunneling conditions. (i) Differences in the local  $C_{60}$  environment may induce a modification of the mixed character of the states and/or a relaxation of the selection rules, as observed in ensemble-averaged experiments [11, 12, 13, 14, 15, 16, 17, 18, 19, 28]. Novel, here, is the fact that the influence of the environment is probed on an individual selected molecule. (ii) Even for equal nominal tunneling parameters, the actual tunneling conditions can vary from one measurement to the other. Tip shape and composition, current instabilities, or electric field fluctuation may influence the relaxation paths, for example by enhancing the intersystem crossing, and increasing the population of the triplet states. The identification of the physical origin of the observation of both, fluorescence and phosphorescence calls for future time-resolved luminescence studies employing both, non-local laser excitation and local STM-induced excitation of supported molecules.

To summarize, unambiguous chemical identification of individual  $C_{60}$  molecules is obtained via their luminescence induced by tunneling electrons. Emission from three electronic states mapping more than twenty vibrational Jahn-Teller and Herzberg-Teller modes of the molecule is identified, in excellent agreement with the

known energies of the electronic [11, 12, 13, 14, 15, 28] and vibrational [14, 21, 27] levels of  $C_{60}$ . The present observation of local fluorescence and phosphorescence demonstrates the capability of STM-induced light emission for the chemical recognition on the single-molecular scale.

The financial support of the Swiss National Science Foundation is acknowledged.

- 
- [1] J. K. Gimzewski, B. Reihl, J. H. Coombs, and R. R. Schlittler, *Z. Phys. B Cond. Matter* **72**, 479 (1988).
  - [2] R. Berndt, J. K. Gimzewski, and P. Johansson, *Phys. Rev. Lett.* **67**, 3796 (1991).
  - [3] R. Berndt, J. K. Gimzewski, and P. Johansson, *Phys. Rev. Lett.* **71**, 3493 (1993).
  - [4] N. Nilius, N. Emst, and H.-J. Freund, *Phys. Rev. Lett.* **84**, 3994 (2000).
  - [5] S. F. Alvarado et al., *J. Vac. Sci. Technol. B* **9**, 409 (1991).
  - [6] G. H. Hoemann, J. K. Liever, and R. Berndt, *Phys. Rev. Lett.* **87**, 176803 (2001).
  - [7] X. H. Qiu, G. V. Nazin, and W. Ho, *Science* **299**, 542 (2003).
  - [8] Z.-C. Dong et al., *Phys. Rev. Lett.* **92**, 086801 (2004).
  - [9] R. Berndt et al., *Science* **262**, 1452 (1993).
  - [10] Z.-C. Dong et al., *Thin Solid Films* **438-439**, 262 (2003).
  - [11] W.-C. Hung, C.-D. Ho, C.-P. Liu, and Y.-P. Lee, *J. Phys. Chem.* **100**, 3927 (1996).
  - [12] A. Sassara, G. Zerza, and M. Chergui, *Chem. Phys. Lett.* **261**, 213 (1996).
  - [13] A. Sassara, G. Zerza, and M. Chergui, *J. Phys. B* **29**, 4997 (1996).
  - [14] A. Sassara et al., *J. Chem. Phys.* **107**, 8731 (1997).
  - [15] D. J. van den Heuvel et al., *Chem. Phys. Lett.* **231**, 111 (1994).
  - [16] D. J. van den Heuvel et al., *J. Phys. Chem.* **99**, 1164 (1995).
  - [17] W. Guss et al., *Phys. Rev. Lett.* **72**, 2644 (1994).
  - [18] D. J. van den Heuvel et al., *Chem. Phys. Lett.* **233**, 284 (1995).
  - [19] I. Akinoto and K. Kan'no, *J. Phys. Soc. Jap.* **71**, 630 (2002).
  - [20] F. Negri, G. Orlandi, and F. Zerbetto, *J. Chem. Phys.* **97**, 6496 (1992).
  - [21] G. Orlandi and F. Negri, *Photochem. Photobiol. Sci.* **1**, 289 (2002).
  - [22] E. I. Altman and R. J. Colton, *Surf. Sci.* **295**, 13 (1993).
  - [23] Y. Saito et al., *Phys. Rev. B* **46**, 1846 (1992).
  - [24] K. Meguro et al., *Phys. Rev. B* **65**, 165405 (2002).
  - [25] R. W. Lof et al., *Phys. Rev. Lett.* **68**, 3924 (1992).
  - [26] S. W. Wu et al., *Phys. Rev. Lett.* **93**, 236802 (2004).
  - [27] V. Schettino, P. R. Salvi, R. Bini, and G. Cardini, *J. Chem. Phys.* **101**, 11079 (1994).
  - [28] M. Chergui, submitted to *Chem. Phys. Lett.*
  - [29] G. Gensterblum et al., *Phys. Rev. Lett.* **67**, 2171 (1991).
  - [30] I. Laszlo and L. Udvardi, *J. Mol. Struct.* **183**, 271 (1989).